frontiers in Forests and Global Change

ORIGINAL RESEARCH
published: 19 July 2021
doi: 10.3389/ffgc.2021.657850

Bark Effects on Stemflow Chemistry in a Japanese Temperate Forest II. The Role of Bark Anatomical Features

Ayano Oka[1], Junko Takahashi[2], Yoshikazu Endoh[3] and Tatsuyuki Seino[2,4]*

[1] Graduate School of Life and Environmental Sciences, University of Tsukuba, Tsukuba, Japan, [2] Faculty of Life and Environmental Sciences, University of Tsukuba, Tsukuba, Japan, [3] Ikawa Forest Station, Mountain Science Center, University of Tsukuba, Shizuoka, Japan, [4] Yatsugatake Forest Station, Mountain Science Center, University of Tsukuba, Minamimaki, Japan

OPEN ACCESS

Edited by:
Anna Klamerus-Iwan, University of Agriculture in Krakow, Poland

Reviewed by:
John T. Van Stan, Georgia Southern University, United States
Salli F. Dymond, University of Minnesota Duluth, United States
Wojciech Piaszczyk, University of Agriculture in Krakow, Poland

***Correspondence:**
Ayano Oka
sbtn.notchi@gmail.com

Specialty section:
This article was submitted to Forest Hydrology, a section of the journal Frontiers in Forests and Global Change

Received: *24 January 2021*
Accepted: *21 June 2021*
Published: *19 July 2021*

Citation:
Oka A, Takahashi J, Endoh Y and Seino T (2021) Bark Effects on Stemflow Chemistry in a Japanese Temperate Forest II. The Role of Bark Anatomical Features. Front. For. Glob. Change 4:657850. doi: 10.3389/ffgc.2021.657850

A fraction of rainfall drains to the soil surface down tree stems (as "stemflow"), and the resulting stemflow waters can be highly enriched with dissolved nutrients due to prolonged bark contact. To date, stemflow chemistry has been examined mostly in regards to the external morphology of the bark, while its relationship with bark anatomy has received little attention. Arguably, this represents a major knowledge gap, because bark anatomical traits are linked to the storage and transport of soluble (and insoluble) organic materials, and control the proximity of these materials to passing stemflow waters. To initiate this line of investigation, here, we examine bark-water leaching rates for common leachable macronutrient ions (Mg^{2+}, Ca^{2+}, and K^{+}) across six different tree species with varying bark anatomical traits (four deciduous broadleaved and two evergreen coniferous species). These different bark types were subjected to laboratory experiments, including observations of bark anatomy and soaking experiments. Laboratory-derived estimates of leaching rates for Mg^{2+}, Ca^{2+}, and K^{+} were then analyzed alongside bark anatomical traits. Leaching rates of Mg^{2+} and Ca^{2+} appear to be controlled by the thickness of the rhytidome and periderm; while K^{+} leaching rates appeared to be driven by the presence of cellular structures associated with resource storage (parenchyma) and transfer (sieve cells). Other species-specific results are also identified and discussed. These results suggest that the anatomical features of bark and the concentration of leachable macronutrient ions in stemflow are related, and that these relationships may be important to understand nutrient cycle through the bark. We also conclude that future work on the mechanisms underlying stemflow solute enrichment should consider bark anatomy.

Keywords: bark anatomy, bark morphology, forest hydrology, rainfall, stemflow

INTRODUCTION

> "L'écorce est une fiere travailleuse"
> [1]"The bark is a proud worker" (Fabre, 1867).

The bark, or the outermost part of the tree stem, is the boundary between the stem and its surrounding environment. This bark boundary protects the internal stem tissues from invasion dryness, fire, and severe external temperatures (Rosell et al., 2014; Pausas, 2015). Bark also plays important roles in forests as an intermediary between the outside environment and the inside of the tree, e.g.: hosting lichens and other corticolous epiphytic life, acting as an exchange site for aerosols and substances within precipitation, and being a pathway for rainfall that drains to the surface as stemflow (Van Stan et al., 2021). Stemflow may also be highly enriched in solutes, resulting in significant, locally concentrated nutrient inputs (Dovey et al., 2011; Germer et al., 2012). Past studies suggested that the amount of stemflow and its solute concentration are strongly coupled to the traits of the bark over which stemflow must drain (Levia and Germer, 2015).

Stemflow chemistry can be influenced by bark contact in several ways. Externally, stemflow can wash off aerosols that were deposited on the bark surface between storms (Levia et al., 2011). The amount of materials captured on the bark varies with the external bark structure–where rough bark on stems, for instance, has been observed to capture nearly 10 times more particles (by mass) than the same area of smoother branch bark surfaces (Xu et al., 2019). There are several studies that have examined the interactions between stemflow chemistry and bark surface structure (Levia and Germer, 2015), and this was the topic for the first part of our research (Oka et al., 2021). Within the bark, however, there are concentrated intracellular solutions that the draining stemflow waters may be able to leach (Klemm et al., 1989). Past work suggests that bark contact may preferentially increase leaching of NH_4^+, K^+, NO_3^-, SO_4^{2-}, and H^+, with the degree of leaching being dependent on bark structure (André et al., 2008). As the bark is capable of taking up external waters, it can also take up solutes (André et al., 2008). The ability for draining stemflow to leach solutes from the bark may depend on bark anatomy, but this has not been investigated to our knowledge. Thus, this manuscript details research that continues from Oka et al. (2021), examining relationships between bark external anatomical traits and stemflow chemistry. Oka et al. (2019, 2021) suggested that Cl^- and Na^+, which are thought to be derived from dry deposition on the tree surface, are easily washed away in the stemflow of smooth bark, while species with coarsely split bark are more likely to leach cations and organic matter, especially Mg^{2+}, Ca^{2+}, and K^+. The external morphology of bark makes a significant contribution to the solute composition and concentration of stemflow, while the thickness and internal morphology of bark are also expected to affect the mechanisms of this bark-water solute exchange. Thus, the anatomical point of view is important for exploring the mechanism of stemflow chemistry (Levia and Herwitz, 2005; Van Stan et al., 2021).

The purpose of this study is to examine how solute leaching [focusing on Mg^{2+}, Ca^{2+}, and K^+ per the results of Oka et al. (2021)] relates to bark anatomical differences among six study tree species in Japan to evaluate bark functions in the exchange of macronutrient cations with stemflow. To accomplish this aim, laboratory experiments were designed to observe the amount, timing, and rates of different solutes leached from the surface of various types of bark. Anatomical observations of the bark were also made to gain insight into the possible connections between bark physiological structures and interspecies solute leaching differences.

MATERIALS AND METHODS

Target Species

The target species were selected according to their bark morphology by moderate, roughness, coarse, and with or without longitudinal tear as following a previous study by Oka et al. (2021). The smooth and mottled bark surface types was represented by *Clethra barbinervis* Sieb. et Zucc.; whereas, the smooth, lateral bark surface types was represented by *Padus grayana* (Maxim.) C. K. Schneid. A moderate bark roughness type was represented by *Magnolia obovata* Thunb. Coarse and deep longitudinal tears distinguished *Castanea crenata* Sieb. et Zucc., as a very rough bark structure. These species were deciduous broad-leaved trees. Evergreen conifers were also selected, where moderate bark roughness was represented by *Abies firma* Sieb. et Zucc., and coarse bark morphology was represented by *Tsuga sieboldii* Carr (**Figure 1**).

Sample Collection and Anatomical Observations

Sample collections were carried out in Tashiro, Shizuoka, central Japan (35.307672N, 138.199925E). The site elevation is 966 m a.s.l., the annual rainfall is 3110.1 mm, and the annual mean temperature is 11.4°C (statistical period according to AMeDAS: 1981–2010, Ministry of Land, Infrastructure, Transport, and Tourism Meteorological Agency HP, https://www.data.jma.go.jp/obd/stats/etrn/index.php, last viewed on December 6, 2019). Forest vegetation of the site is mixed forest of deciduous broad-leaved trees and evergreen conifers (Seino and Endoh, 2019). The site is approx. 48 km far from the nearest coast, and the site is surrounded by natural forests, and there are almost no factories or residential area in the area. Therefore, the mineral supply from the ocean (especially Cl^-) and the influence of pollutants (some nitrogen oxides) from human activities are expected to low (**Figure 2**).

Bark samples for anatomical analysis approximately 4 cm^2 were collected at the site in September 2019. This sampling time was selected to minimize the effects of mineral leaching from the bark due to heavy rainfall caused by the Japanese rainy season and typhoons. The samples were obtained from sound individuals with minimal observable surface damage, not covered with lichen or epiphytes, and collected at a height of approx. 1 m above the ground using a chisel. The thickness of each bark sample was measured at three points using a manual caliper. Anatomical analysis was carried out in the laboratory of the Yatsugatake Forest Station, Mountain Science Center,

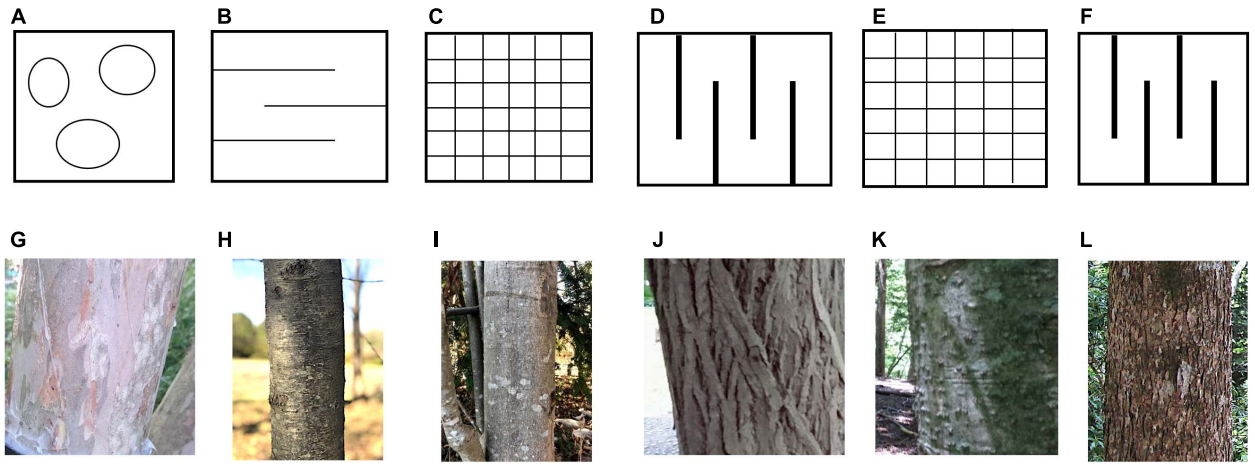

FIGURE 1 | Schematic diagram of bark surface and photographs of the bark of target tree species. The upper row is a schematic drawing of the bark surface, **(A)** smooth and mottled surface type, **(B)** smooth lateral skin type, **(C)** moderate roughness type, **(D)** coarse and deep longitudinal tear type, **(E)** moderate type of conifer, and **(F)** coarse type of conifer. The middle row shows bark photographs of the trees in which soaking experiments of the bark were conducted, **(G)** *Clethra barbinervis,* **(H)** *Padus grayana,* **(I)** *Magnolia obovata,* **(J)** *Castanea crenata,* **(K)** *Abies firma,* and **(L)** *Tsuga sieboldii.*

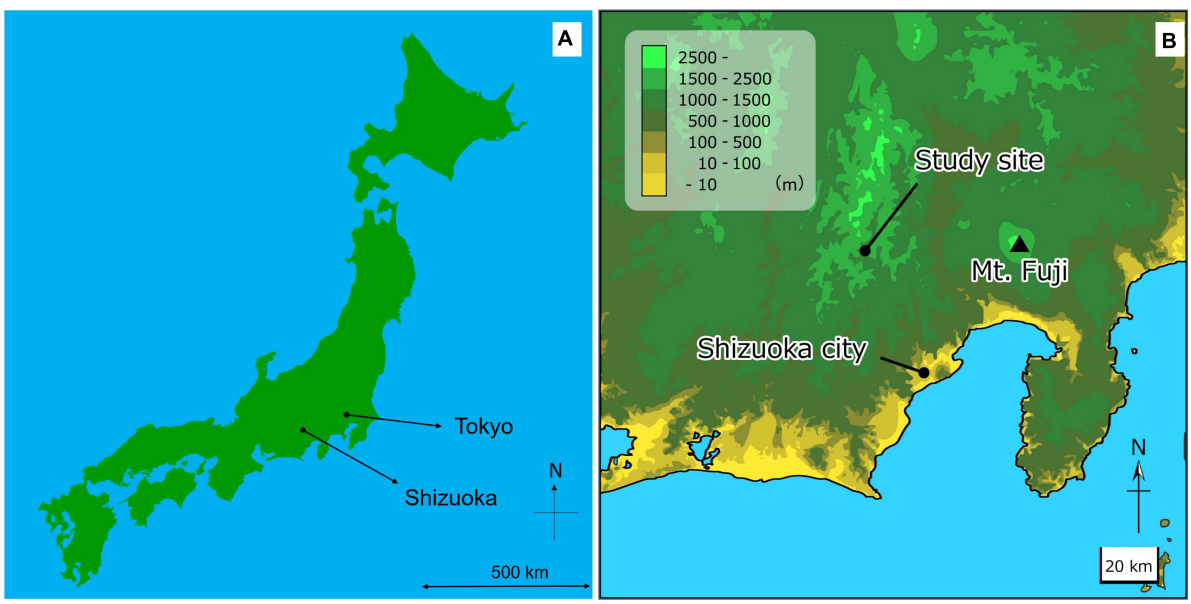

FIGURE 2 | Map of the sample collection area. **(A)** Map of Japan, and **(B)** Map of around the sample collection site.

University of Tsukuba, Japan. The bark samples were fixed and softened in 99.5% ethanol, and lateral sections were prepared using a sliding microtome (TU-213, Yamato Kohki Industrial, Saitama, Japan). Cross sections (30 μm thick) were obtained from the bark samples. Cross sections were dehydrated in an ethanol series and sequentially stained with safranin and methyl blue. Permanent preparations were made for observations of the morphology and arrangement of the cells with an optical microscope (BX53, Olympus, Tokyo, Japan), and anatomical photographs were taken with a digital camera (EOS Kiss X7i, Canon, Tokyo, Japan).

The general structures of bark were defined as follows (Shimaji et al., 1976; Trockenbrodt, 1990; Angyalossy et al., 2016). The bark encompasses all of the tissues outside the cambium of a tree. It is broadly divided from the outside into the epidermis, periderm, cortex, and secondary phloem. The epidermis, the outermost cell with a thick cell wall, is responsible for preventing water loss from inside the tree and protecting the tree body from external stimuli. The periderm, which serves as secondary lateral meristem to the disrupted epidermal layer, consists of phellem, phellogen, and phelloderm. The cortex is the foundation of the periderm. The secondary phloem includes radiation tissue–which

is responsible for the transport of materials and for their storage– as well as bast fiber and sclereids–which provide mechanical strength. According to the above definitions, the anatomical findings of the bark structures of each species are described.

Bark-Soaking Experiment

Bark samples for soaking experiments were collected at the site in September 2019, with three bark samples of approximately 9 cm^2 from each, for a total of 18 samples at the laboratory of University of Tsukuba, Japan. The reason for the sample size was that there was a limit to the number of individuals suitable for bark collection and due to the time constraint in the process of immersion experiments. The inner surfaces and sections of the bark samples were coated with paraffin wax and soaked for the first time in 200 ml of distilled water after 12 h. The samples were placed in a petri dish so that the outer bark was immersed in water. The water samples were collected continuously throughout the soaking experiment by removing 4 ml samples from the petri dish every 24 h. The soaking time was set to maximum at 96 h due to the expectation that the extracted minerals would reach at a saturation concentration by that time. The concentrations of target inorganic ions (Mg^{2+}, Ca^{2+}, and K^{+}) were measured in a total of 90 water samples using ion chromatography (Prominence series, Shimadzu, Kyoto). Calibration curves were tested using five mixed standard solution for the peak area of each ion and organic carbon, and quantification was performed after confirming their correlation coefficients. The reproducibility of the peak area, was regularly confirmed that the CV is 2% or less.

Data Analysis

To evaluate patterns leaching cations from the bark, we applied a Principal Components Analysis using the online ClustVis application[1] by Metsalu and Vilo (2015). A PCA analysis was performed to explore possible interrelations of K^{+}, Mg^{2+}, and Ca^{2+} leaching rates with bark anatomical traits.

RESULTS

Anatomical Findings of Species

According to the above-mentioned definitions by Shimaji et al. (1976); Trockenbrodt (1990), and Angyalossy et al. (2016), the anatomical findings of the bark structures of each bark type by species are described and summarized in **Table 3**. Anatomical pictures are included in the **Supplementary Figures**. The bark surface morphology was already described in a previous research by Oka et al. (2021).

The smooth and mottled bark of *Clethra barbinervis* has a thin cortex from the epidermis and well-developed radiating tissue that is distinct (**Table 3**). We observed a raised epidermis over the extension of the radiation tissue. The epidermis of *Padus grayana* has a thin cork phelloderm on the periderm that forms a linear rhytidome. Gaps are also common at the border between the cortex and the secondary phloem for *P. grayana*. This species radiation tissue is developed in three to five rows of cells, and there are gaps along this radiation tissue as well. Parenchyma were also observed in a distinct, cross-sectional direction for *P. grayana*. For the moderately-rough barked *Magnolia obovata*, the epidermis is mostly absent, with uneven, slightly developed phellem. The *M. obovata* cortex has a rare supra-grain sclereid, is spongy with many gaps, and characterized by the expansion and development of the radiation tissue toward the cortex in the middle of the secondary phloem. Circumferential parenchyma and bast fibers are also well developed and distinct in the *M. obovata* samples. The coarse, deep, longitudinal tears of *Castanea crenata* bark is related to a wave-patterned periderm that forms its rhytidome. A thin radiation tissue consisting of one or two rows of cells was found in the secondary phloem of *C. crenata*. This species also has thick bast fibers alternating with parenchyma at equal intervals. Bark of the conifer, *Abies firma*, shows several layers of thin, smooth periderm overlap with a thickly developed mosaic-like layer of skin mixed with live cells and sclereids. There were also many gaps in *A. firma* samples, which was common in the broadleaved moderate bark (i.e., *M. obovata*). The secondary phloem of *A. firma* is thinner than that of the other broad-leaved trees, and the radiation tissue is thin and indistinct. The coarse bark conifer, *Tsuga sieboldii*, has an outer rhytidome and porous bark layer that appears similar to *A. firma*. The old periderm of *T. sieboldii* has scattered ball-shaped sclerae, while the inner new phelloderm is wavy and well-developed. The parenchyma of the secondary phloem of this species indistinctly intrudes into the cortex and are characterized by the presence of many clustered sclereids.

Bark-Soaking Experiment

For minerals leaching from a tree body, such as K^{+}, Ca^{2+}, and Mg^{2+}, their concentrations differed among species and with soaking time (**Figure 3** and **Table 1**). All studied cations increased until settling near the maximum (i.e., 96-h) concentration (**Figure 3** and **Table 2**). Mg^{2+} concentrations tended to be low in *Padus grayana* (7.64–39.61 μmol L^{-1}), *T. sieboldii* (5.12–25.42 μmol L^{-1}), *A. firma* (13.25–30.61 μmol L^{-1}), and *C. barbinervis* (8.39–29.05 μmol L^{-1}), but concentrations of Mg^{2+} were generally higher in *M. obovata* (24.56–88.57 μmol L^{-1}) and *C. crenata* (24.62–34.03 μmol L^{-1}) (ANOVA, $F_{[5,58]} = 5.19$, $p < 0.001$ by species). For all trees,

TABLE 1 | Leaching rates (μmol L^{-1} h^{-1}) of K^{+}, Mg^{2+}, and Ca^{2+} by species, estimated as the slope of a linear regression relating concentration and time of saturation during the soaking experiment.

Species	K^{+}		Mg^{2+}		Ca^{2+}	
	Mean	Range	Mean	Range	Mean	Range
Clethra barbinervis	0.40	0.15–0.53	0.18	0.10–0.28	0.32	0.09–0.74
Padus grayana	0.53	0.29–0.77	0.17	0.08–0.25	0.28	NA
Magnolia obovata	2.11	0.24–3.51	0.27	0.23–0.28	0.75	0.71–0.79
Castanea crenata	0.19	0.15–0.24	0.50	0.20–0.90	1.01	0.35–1.48
Abies firma	1.85	0.26–2.84	0.19	0.07–0.35	0.26	0.09–0.70
Tsuga sieboldii	0.70	0.19–1.64	0.15	0.05–0.23	0.23	0.20–0.26

[1]https://biit.cs.ut.ee/clustvis/

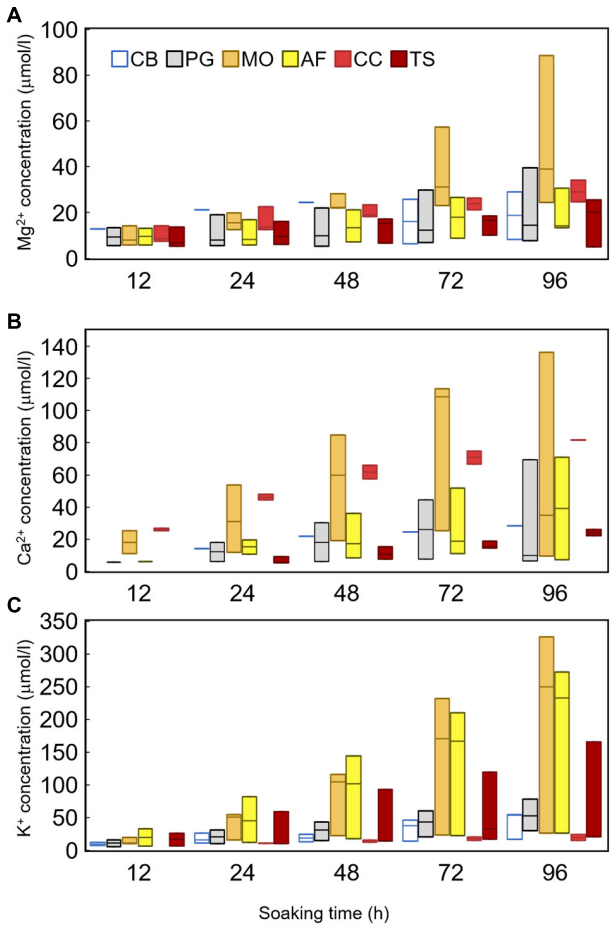

FIGURE 3 | Box-plot of concentrations of inorganic ion, **(A)** Mg^{2+}, **(B)** Ca^{2+}, and **(C)** K^{+} extracted from the bark by soaking experiment. Colors mean each species as *Clethra barbinervis* (white), *Padus grayana* (gray), *Magnolia obovata* (orange), *Abies firma* (yellow), *Castanea crenata* (light red), and *Tsuga sieboldii* (deep red). Bars in figure are SD.

Mg^{2+} concentrations increased over time of the soaking experiment, especially for *M. obovata* (**Figure 4**). Concentrations of Ca^{2+} in *A. firma* (7.04–71.07 μmol L^{-1}) and *C. crenata* (81.77 μmol L^{-1}) were higher than those for other species (**Figure 4**). In *M. obovata*, Ca^{2+} concentrations were lower and often undetectable in some samples. Up to 48 h, *C. crenata* had the highest concentrations of Ca^{2+} (57.34–74.73 μmol L^{-1}), after which its concentration exceeded those of *M. obovata* during the same soaking times [ANOVA, $F_{(5,42)} = 4.66$, $p < 0.01$ by soaking time]. The highest concentrations of K^{+} were, in order, *M. obovata* (26.22–325.74 μmol L^{-1}), *A. firma* (26.19–232.85 μmol L^{-1}), *T. sieboldii* (20.38–165.23 μmol L^{-1}), *P. grayana* (29.76–77.99 μmol L^{-1}), *C. barbinervis* (16.79–54.20 μmol L^{-1}), and *C. crenata* (15.08–24.47 μmol L^{-1}). For all tree species, K^{+} concentrations increased over time, while in the same order [ANOVA, $F_{(4,53)} = 6.16$, $p < 0.001$ by soaking time] (**Figure 4**). As for the leaching rate and their linearity along a time course, there were no remarkable relations. The bark types such as *C. crenata* and *T. sieboldii* tended to leach more easily than others (**Tables 2**, **3**).

Two principal components were identified that represented ∼60% of the variability within these data: 37% in component 1 (PC1) and 23% in component 2 (PC2). The three bark samples from each species (indicated by symbol color) clustered together across the PC space; however, these species-specific clusters are generally distinct from each other (**Figure 5**). The loadings (lower right) suggest that the leaching rates of Mg^{2+} and Ca^{2+} across the studied tree species may be possibly driven by similar anatomical features of the bark. Specifically, Mg^{2+} and Ca^{2+} leaching rates load alongside the rhytidome thickness (Rhy), periderm thickness (Per), and the presence of bast fibers (Bst) (**Figure 5**). K^{+} leaching rates, on the other hand, seem to be influenced by the presence of cavities (Cav), parenchyma (Par), sieve cells (Siv), and cortical thickness (Ctx) (**Figure 3**). The spread among species and their clusters in the PCA plot is larger along the direction of loading by K^{+} and its affiliated bark anatomical features (i.e., from quadrants 2 to 4), compared to the influence of Mg^{2+} and Ca^{2+} leaching rates/bark features (**Figure 5**). The exception to this is *A. firma*, for which one of the samples plotted relatively far from the other two samples in both major loading directions.

DISCUSSION

Comparison of Anatomical Structures by Bark Type

From the results of this study, the anatomical characteristics of the inner bark are not simply determined by the thickness of the outer bark, which is often how comparisons have been drawn between solute concentrations and their sources in the rain waters that have drained through tree canopies (Levia and Frost, 2003; Levia and Germer, 2015; Lu et al., 2017; Oka et al., 2021). These anatomical descriptions and the assessment of their interactions with the select macronutrient cations in this study may provide a roadmap for future work on the biogeochemical interactions between bark and stemflow or branchflows. Many of the anatomical structures identified in this study are analogous to other species' bark. The structure of the *P. grayana* periderm, for example, which contains a thin, smooth, lateral phellem has also been observed in *Betula platyphylla* Sukaczev var. *japonica* (Miq.) H. Hara (Shibui and Sano, 2018) which bark surface is

TABLE 2 | Coefficients of the relationship between time and percentage of maximum concentration over the soaking experiment.

Species	K^{+}	Mg^{2+}	Ca^{2+}
Clethra barbinervis	0.93*	0.93**	0.93***
Padus grayana	0.97***	0.97***	0.79**
Magnolia obovata	0.89*	1.01***	0.89**
Castanea crenata	0.72*	0.84*	0.92***
Abies firma	0.90**	0.95***	0.88**
Tsuga sieboldii	0.95**	0.54*	0.90***

*Asterisks denote p value (*p < 0.05; **p < 0.01; ***p < 0.001).*

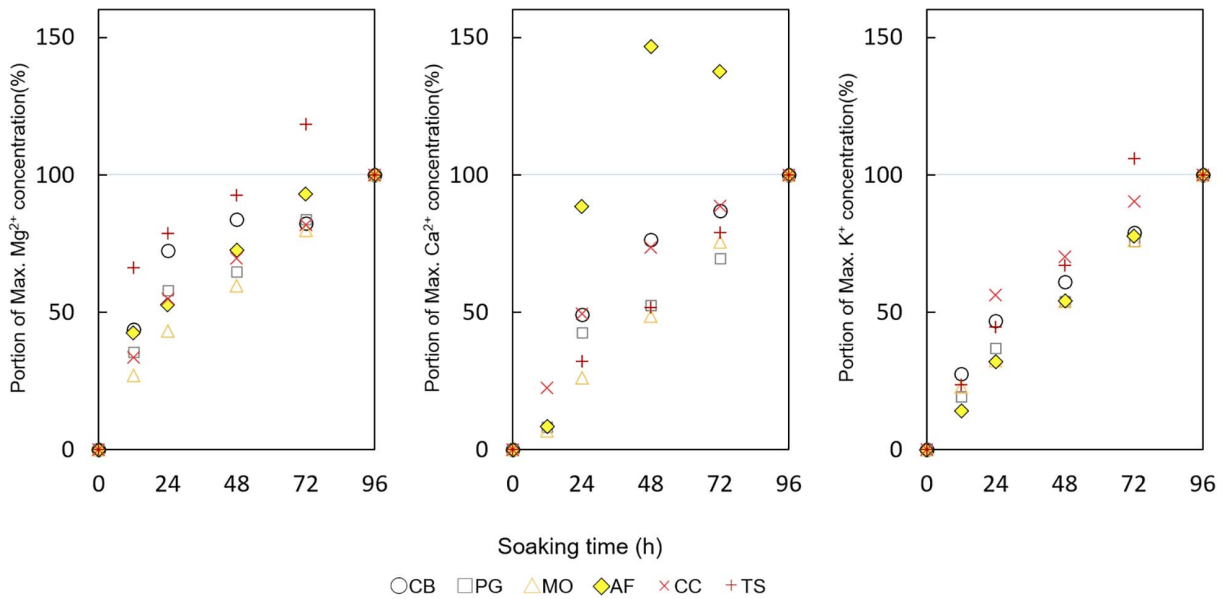

FIGURE 4 | The portions of maximum Mg^{2+}, Ca^{2+}, and K^{+} concentration (%) by soaking time (hr). Colors mean each species as CB *Clethra barbinervis* (white circle), PG as *Padus grayana* (gray square), MO as *Magnolia obovata* (orange triangle), AF as *Abies firma* (yellow diamond), CC as *Castanea crenata* (light red x), and TS as *Tsuga sieboldii* (deep red cross).

similar to that of *P. grayana*. Some bark anatomical traits were similar across coniferous and broadleaved study species. For the moderately rough bark types, such as *M. obovata* and *A. firma*, both had gaps and sclereids at the border between the periderm and the secondary phloem. The bark of these moderate types was also similar to that of *P. grayana* except for the characteristics of the periderm. The coarse, deep, longitudinal structure of the thick rhytidome and the structure of the secondary phloem were similar in both *C. crenata* and *T. sieboldii*. Some features were only observed in one of the species. For example, the characteristically well-developed radiation tissue was observed only in *M. obovata*. Across the studied species, however, the internal anatomy of smooth, moderate, and coarse bark types did differ greatly.

These different bark anatomies suggested that the possible solute exchange between the bark and the drained rainwater is related to tree growth. For example, Shibata and Sakuma (1996) and Staelens et al. (2007) have shown that seasonal changes in the dynamics of the chemistry of deciduous broadleaf tree stemflow were related to tree growth, especially leaf phenology such as leaf flush, expansion, and defoliation. Carmo et al. (2016) analyzed minerals in the bark of *Copaifera langsdorffii* Desf. (Fabaceae) by correlating chemical analysis with anatomical characteristics. Carmo et al. (2016) also analyzed the relationship between bark anatomies such as its thickness and the mineral source within each tissue. The results of this study provide a prospect to explore the mechanisms of solute enrichment by bark-water interactions from the following soaking experiments.

Bark-Soaking Experiment

A trend of increasing concentration over soaking time was observed for all species' bark samples for Mg^{2+}, Ca^{2+}, and K^{+}, which are solubilizing substances. For Mg^{2+} and Ca^{2+}, the concentrations of *C. crenata* were high up to 24 h later–and at similar concentrations to those of stemflow samples from the field (Oka et al., 2021); however, after 48 h, the concentrations were higher in *M. obovata*. This suggests that the bark of *M. obovata* is particularly prone to the accumulation of substances, and that there may be a time lag in the leaching of these cations to water contacting the bark. We note that the residence time of rainwater on bark may be exaggerated in our soaking experiments; however, to our knowledge, no residence time estimates for stemflow in tree canopies currently exist. Thus, there are no observations or estimates of the appropriate time duration that one could have used to guide the soaking experiment. We assume that the length of our soaking experiment represents a maximum residence time, yet storms may last several days and snow residence time on bark (before melt) may last 96 h or longer (Klamerus-Iwan et al., 2020). It may be that the amount of cation accumulation that is leachable during these soaking experiments was related to the internal structure of the bark, such as the cortex, rather than the surface structure.

Much attention has been focused on the water storage capacity of bark (Levia and Herwitz, 2005; Van Stan et al., 2016) and its function as a source of minerals (Wetzel and Greenwood, 1989; Wetzel et al., 1989; Wolterbeek et al., 1996). In the case of those bark-derived leaching cations examined in this study (Ca^{2+}, Mg^{2+}, and K^{+}), Ca^{2+} tended to be more abundant in tree bodies (Jones et al., 2019), while Mg^{2+} and K^{+} tend to be more concentrated in leaves, which is closely related to their physiological in individual trees (Shibata and Sakuma, 1996; Jones et al., 2019). It has been suggested that the leaching of these cations from tree body is related to the water-storage function of the bark because, hypothetically,

TABLE 3 | Summarized of anatomical characteristics of each species.

			Anatomical characteristics										
	Bark morphology		**Species**		**Perderm**			**Cortex**		**Secondary phloem**			
			Thickness (mm)	**Epodermis**		**(apr. mm)**	**Rhytidomes**		**(apr. mm)**	**Sclereid**	**Radiation tissue**	**Sieve cell**	**Parenchyma**	**Bast fiber**
Broad-leaved trees	Smooth and mottled surface	*Clethra barbinervis*	0.54 ± 0.05^{a}	Very thin	Very thin	0.02	×	Very thin	0.065	×	Well-developed	Scatter	×	×
	Smooth with lateral skin	*Padus grayana*	3.69 ± 0.20^{ac}	×	Horizontal straight	0.44	Thin pericarp layered	Cavity	0.39	×	Well-developed	Well-developed	Circumferential	×
	Moderate roughness	*Magnolia obovate*	6.08 ± 0.36^{cd}	×	Slightly developed	0.26	Mono layered	Many cavities	1.17	○	Expanding outward	Obscure	Well-developed	Well-developed
	Coarse and deep longitudinal tear	*Castanea crenata*	6.57 ± 1.48^{cd}	×	Developed	1.96	Wavy development, layered	Thin	0.26	×	Narrow	Well-developed	Well-developed	○
Conifers	Moderate roughness	*Abies firma*	6.53 ± 0.40^{cd}	×	Thin	0.39	Thin pericarp overlaps	Mosaic with cabity	5.33	○	×	×	Obscure	×
	Coarse and deep longitudinal tear	*Tsuga sieboldii*	6.29 ± 0.59^{bcd}	×	Thick outside thick inside	0.39	Wavy development	Mosaic with cabity	0.84	○ Ball shaped develop	×	×	Obscure	×

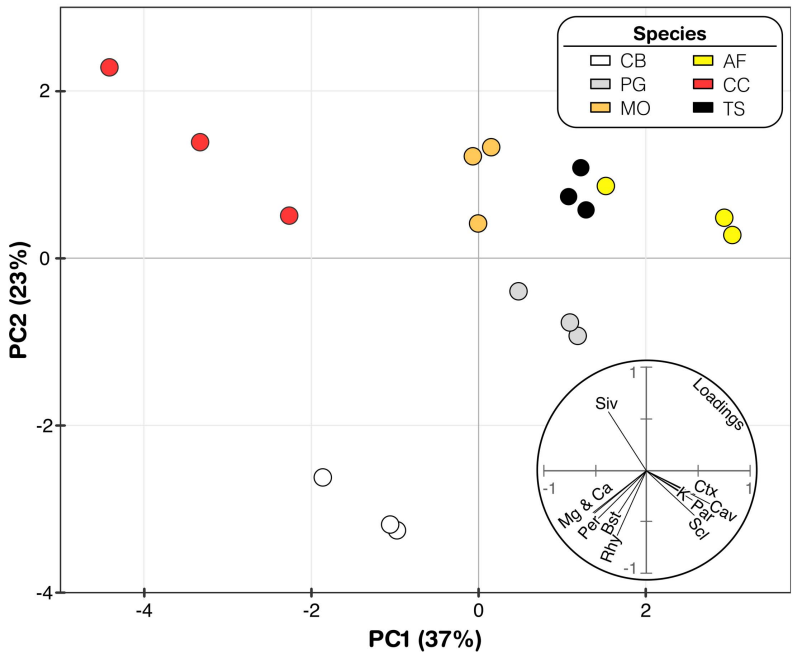

FIGURE 5 | Principal component analysis with Mg^{2+}, Ca^{2+}, and K^{+} concentrations related to anatomical components. The arrows represent variable plotted by the first two PCA axes. Species abbreviations are *Clethra barbinervis* (CB) *Padus grayana* (PG), *Magnolia obovata* (MO), *Castanea crenata* (CC), *Abies firma* (AF), and *Tsuga sieboldii* (TS), respectively.

greater water storage equates to longer bark-water contact times (Levia and Herwitz, 2005; Abbasian et al., 2015). To date, however, the physiological mechanisms of the bark-water interactions that underlie the enrichment of stemflow with the macronutrient ions remain relatively undescribed–especially compared to leaching mechanisms in leaves (Aubrey, 2020). This may be a result of common methods for estimating leaching rates in throughfall and stemflow requiring no knowledge of bark anatomy and physiology, e.g.: (i) multiple regression modeling (Lovett and Lindberg, 1984); (ii) parsing washoff and leaching from intrastorm trends in water chemistry (Kazda and Glatzel, 1986; Kazda, 1990); or (iii) using tracer solutes (Staelens et al., 2008; Turpault et al., 2021). Our results suggest that bark anatomy plays an important role in the leaching of macronutrient cations into waters draining through woody plant canopies.

From the principal components analysis, leaching of Mg^{2+} and Ca^{2+} appears to be driven by similar bark anatomical traits such as a thickness of rhytidome and periderm, as well as bast fibers. The thickness of the rhytidome and periderm may influence these leaching rates by influencing the distance between living cells (beyond the rhytidome) and the stored or draining rainwaters (as similarly hypothesized by André et al., 2008). Given that bast fibers primarily provide stabilizing or mechanical support functions, it's relationship with the leaching of Mg^{2+} and Ca^{2+} is uncertain. K^{+} appears to be driven by the presence of cavities, parenchyma, sieve cells, sclereids and cortex thickness. The statistical inference of a relationship between K^{+} leaching rates and some of these anatomical features seems reasonable, particularly given that parenchyma are generally specialized storage tissue (which may hold a variety of materials, like starches, oils, resins, etc.: Zabel and Morrell, 2020), and that sieve cells may conduct sugars and can be associated with parenchyma (Simpson, 2019). Bark anatomical results by Carmo et al. (2016), observed cavities, sclereids, cortex thickness of *C. langsdorfifii* bark, and detected chemical composition in the fractionation of extractives. K^{+} plays an important role in photosynthesis, ion transport, and osmotic adjustment in plants. Therefore, it would be important to know that K^{+} compartments present and related to their ecophysiological activity, and the thickness of the sclerotium as its storage function. In addition, since sclereids are formed by changes in old sieve cells, if the relationship between the process of formation and the concentration of K^{+} is detected it can be expected to indicate the process of bark development and the physiological activity at the crown through the chemistry of the stemflow.

Although our study focused on K^{+}, Mg^{2+}, and Ca^{2+}, there are other solutes meritorious of investigation with regard to their bark-water interactions. Wetzel et al. (1989) reported on the nitrogen storage function of bark from the perspective of bark anatomy. Past research on the composition of organic chemical components in *Pinus densiflora* Siebold and Zucc., bark aimed at the effective use of bark as a residue of timber production (Hata and Sogo, 1956). Others have examined tannin extraction from the bark of species useful for wood (Ohara, 2009). For one of the target tree species in this research, past work has examined essential oil components in the bark of

M. obovata (Fujita et al., 1973). Research on the bark of *Fraxinus lanuginosa* Koidz. f. *serrata* (Nakai) Murata has also been done for the isolation of naturally occurring antioxidants (Hayafuji, 2018) which may be useful in assessing the quality of medicinal components. Thus, this work builds on a long, but sparse, history of research on bark anatomy and its relationship with water and solutes by shedding new insights into the possible role of bark anatomical traits in the dynamics of inorganic components leached from the bark to stemflow.

CONCLUSION

Current theory on the influence of bark on stemflow chemistry solely considers the influence of external bark surface morphology, neglecting the role of bark anatomy. The results of this study suggest that bark anatomical traits are related to stemflow chemistry for commonly leached macronutrient ions (K^+, Mg^{2+}, and Ca^{2+}) across a wide range of bark types studied here (six species from coniferous and broadleaved trees). These results further suggest that the stemflow-bark interactions can play an important role in the transfer and intrasystem cycling of macronutrients between the inside of the tree and the external environment. Across bark samples of varying anatomy, Mg^{2+} and Ca^{2+} leaching rates were driven by the thickness of the rhytidome and periderm–hypothetically reducing leaching rates as the distance between living cells (beyond the rhytidome) and stemflow is increased. K^+ leaching rates appeared to be driven by the presence of anatomical features associated with resource storage (parenchyma) and transfer (sieve cells). For some bark types, such as *Abies firma* and *Magnolia obovata*, that had a spongy anatomy, with gaps were found at the boundary between the epidermis and the secondary phloem that appear to delay bark-stemflow solute exchange. The concentrations of tree body derived leachates were higher in the stemflow of study trees like *Castanea crenata* and *Tsuga sieboldii*, suggesting that the rhytidome thickness and the presence or absence of sieve cells and associated parenchyma are related. Even in the coarse bark type, there was a difference in the internal structure between conifers and hardwoods, which may have resulted in a difference in the tendency of the stemflow chemistry. We recommend that future work seeking to mechanistically explain variability in stemflow solute concentration, composition, and especially leaching from bark surfaces, examine bark anatomical traits.

DATA AVAILABILITY STATEMENT

The original contributions presented in the study are included in the article/**Supplementary Material**, further inquiries can be directed to the corresponding author.

AUTHOR CONTRIBUTIONS

All authors conceived and designed the research plan. AO, YE, and TS collected the samples. AO and JT carried out chemical analyses. AO and TS operated anatomical analyses. All authors contributed to the manuscript writing.

FUNDING

This study was partly supported by a Grant-in-Aid from the Mountain Research Center, University of Tsukuba.

ACKNOWLEDGMENTS

We are grateful to reviewers, Anna Klamerus-Iwan, John Van Stan, Yoshihiko Tsumura, Takashi Kamijo, and laboratory member of Ikurinken for their fruitful advice; Shozo Kato of Kato Limited Partnership Company and staff member of the Ikawa Forest Station, Mountain Research Center, University of Tsukuba for kind support during fieldwork. Miho Sato for providing the photograph of *Juglans mandshurica* var. *sachalinensis* in **Figure 1**.

SUPPLEMENTARY MATERIAL

The Supplementary Material for this article can be found online at: https://www.frontiersin.org/articles/10.3389/ffgc.2021.657850/full#supplementary-material

Supplementary Figure 1 | Cross-section pictures of *Clethra barbinervis*. Abbreviations for anatomical terms are described in the anatomical observations section of the text; epidermis (ep), periderm (pd), phelloderm (pld), cortex (cor), secondary phloem (sp), sieve cell (s), and radiating tissue (r). The photograph was taken at 40×.

Supplementary Figure 2 | Cross-section pictures of *Padus grayana.* Abbreviations for anatomical terms are described in the anatomical observations section of the text; periderm (pd), phellem (pl), phellogen (plg), phelloderm (pld), ritidome (rd), cortex (cor), sclereid (sc), origin sclereid (osc), secondary phloem (sp), parenchyma (p), sieve cell (s), and radiating tissue (r). The photograph was taken at 40×. The picture was combined multiple photos.

Supplementary Figure 3 | Cross-section pictures of *Magnolia obovata.* Abbreviations for anatomical terms are described in the anatomical observations section of the text; periderm (pd), phellem (pl), phellogen (plg), phelloderm (pld), ritidome (rd), cortex (cor), sclereid (sc), origin sclereid (osc), secondary phloem (sp), parenchyma (p), sieve cell (s), radiating tissue (r), and bast fiber (f). The photographs were taken at 40×. Picture was combined multiple photos.

Supplementary Figure 4 | Cross-section pictures of *Castanea crenata.* Abbreviations for anatomical terms are described in the anatomical observations section of the text; periderm (pd), ritidome (rd), cortex (cor), sclereid (sc), origin sclereid (osc), secondary phloem (sp), parenchyma (p), sieve cell (s), radiating tissue (r), and bast fiber (f). The photograph was taken at 40×. The picture was combined multiple photos.

Supplementary Figure 5 | Cross-section pictures of *Abies firma.* Abbreviations for anatomical terms are described in the anatomical observations section of the text; periderm (pd), ritidome (rd), cortex (cor), sclereid (sc), origin sclereid (osc), secondary phloem (sp), parenchyma (p), and radiating tissue (r). The photograph was taken at 40×. Picture was combined multiple photos.

Supplementary Figure 6 | Cross-section pictures of *Tsuga sieboldii.* Abbreviations for anatomical terms are described in the anatomical observations section of the text; periderm (pd), ritidome (rd), cortex (cor), sclereid (sc), and radiating tissue (r). The photograph was taken at 40×. Picture was combined multiple photos.

REFERENCES

Abbasian, P., Attarod, P., Sadeghi, S. M. M., Van Stan, J. T., and Hojjati, S. M. (2015). Throughfall nutrients in a degraded indigenous Fagus orientalis forest and a Picea abies plantation in the of North of Iran. *Forest Syst.* 24:1. doi: 10.5424/fs/2015243-06764

André, F., Jonard, M., and Ponette, Q. (2008). Effects of biological and meteorological factors on stemflow chemistry within a temperate mixed oak–beech stand. *Sci. Total Environ.* 393, 72–83. doi: 10.1016/j.scitotenv.2007.12.002

Angyalossy, V., Pace, M. R., Evert, R. F., Marcati, C. R., Oskolski, A. A., Terrazas, T., et al. (2016). IAWA list of microscopic bark features. *IAWA J.* 37, 517–615. doi: 10.1163/22941932-20160151

Aubrey, D. P. (2020). *Relevance of precipitation partitioning to the tree water and nutrient balance. In Precipitation partitioning by vegetation*. Cham: Springer, 147–162.

Carmo, J. F., Miranda, I., Quilhó, T., Sousa, V. B., Cardoso, S., Carvalho, A. M., et al. (2016). Copaifera langsdorffii bark as a source of chemicals: structural and chemical characterization. *J. Wood Chem. Technol.* 36, 305–317. doi: 10.1080/02773813.2016.1140208

Dovey, S. B., du Toit, B., and de Clercq, W. (2011). Nutrient fluxes in rainfall, throughfall and stemflow in Eucalyptus stands on the Zululand coastal plain, South Africa. *Southern Forests J. Forest Sci.* 73, 193–206. doi: 10.2989/20702620.2011.639506

Fabre, J. H. (1867). *Histoire de la Bûche - Récits sur la Vie des Plantes*. Whitefish, MT: Kessinger Publishing.

Fujita, M., Itokawa, H., and Sashida, Y. (1973). Studies on the components of Magnolia obovata Thunb. II. On the components of the methanol extract of the bark. *Yakugaku Zasshi* 93, 422–428. doi: 10.1248/yakushi1947.93.4_415

Germer, S., Zimmermann, A., Neill, C., Krusche, A. V., and Elsenbeer, H. (2012). Disproportionate single-species contribution to canopy-soil nutrient flux in an Amazonian rainforest. *Forest Ecol. Manage.* 267, 40–49. doi: 10.1016/j.foreco.2011.11.041

Hata, K., and Sogo, M. (1956). Chemical studies on the bark I. Chemical composition and some chemical properties of the bark of Japanese red pine (Pines densiflora S. et Z.). *J. Jap. Forestry Soc.* 38, 473–478. doi: 10.11519/jjfs1953.38.12_473

Hayafuji, A. (2018). Search of antioxidative constituents of the bark of Fraxinus lanuginosa. *JSSE Res. Rep.* 32, 11–14. doi: 10.14935/jsser.32.8_11

Jones, J. M., Heineman, K. D., and Dalling, J. W. (2019). Soil and species effects on bark nutrient storage in a premontane tropical forest. *Plant Soil* 438, 347–360. doi: 10.1007/s11104-019-04026-9

Kazda, M. (1990). "Sequential stemflow sampling for estimation of dry deposition and crown leaching in beech stands," in *Nutrient cycling in terrestrial ecosystems: field methods, application and interpretation*, eds A. F. Harrison, P. Ineson, and O. W. Heal (London: Elsevier Applied Science), 46–55.

Kazda, M., and Glatzel, G. (1986). *Dry deposition, retention and wash-off processes of heavy metals in beech crowns: Analysis of sequentially sampled stemflow. In Atmospheric Pollutants in Forest Areas*. Dordrecht: Springer, 215–222.

Klamerus-Iwan, A., Lasota, J., and Błońska, E. (2020). Interspecific variability of water storage capacity and absorbability of deadwood. *Forests* 11:575. doi: 10.3390/f11050575

Klemm, O., Kuhn, U., Beck, E., Katz, C., Oren, R., Schulze, E. D., et al. (1989). *Leaching and uptake of ions through above-ground Norway spruce tree parts. In Forest decline and air pollution*. Berlin, Heidelberg: Springer, 210–237.

Levia Jr, D. F., and Frost, E. E. (2003). A review and evaluation of stemflow literature in the hydrologic and biogeochemical cycles of forested and agricultural ecosystems. *J. Hydrol.* 274, 1–29. doi: 10.1016/S0022-1694(02)00399-2

Levia, D. F., and Germer, S. (2015). A review of stemflow generation dynamics and stemflow-environment interactions in forests and shrublands. *Rev. Geophys.* 53, 673–714. doi: 10.1002/2015RG000479

Levia, D. F., and Herwitz, S. R. (2005). Interspecific variation of bark water storage capacity of three deciduous tree species in relation to stemflow yield and solute flux to forest soils. *Catena* 64, 117–137. doi: 10.1016/j.catena.2005.08.001

Levia, D. F., Van Stan, J. T., Siegert, C. M., Inamdar, S. P., Mitchell, M. J., Mage, S. M., et al. (2011). Atmospheric deposition and corresponding variability of stemflow chemistry across temporal scales in a mid-Atlantic broadleaved deciduous forest. *Atmospheric Environ.* 45, 3046–3054. doi: 10.1016/j.atmosenv.2011.03.022

Lovett, G. M., and Lindberg, S. E. (1984). Dry deposition and canopy exchange in a mixed oak forest as determined by analysis of throughfall. *J. Appl. Ecol.* 21, 1013–1027. doi: 10.2307/2405064

Lu, J., Zhang, S., Fang, J., Yan, H., and Li, J. (2017). Nutrient fluxes in rainfall, throughfall, and stemflow in *Pinus densata* natural forest of Tibetan Plateau. *Clean - Soil, Air, Water*. 45, 1–9. doi: 10.1002/clen.201600008

Metsalu, T., and Vilo, J. (2015). ClustVis: a web tool for visualizing clustering of multivariate data using Principal Component Analysis and heatmap. *Nucleic Acids Res.* 43, W566–W570.

Ohara, S. (2009). Chemical characteristics of bark tannis and their chemical and enzymatic conversions. *J. Jap. Wood Res. Soc.* 55, 59–68. doi: 10.2488/jwrs.55.59

Oka, A., Takahashi, J., Endoh, Y., and Seino, T. (2019). Effect of bark characteristics on stemflow and its chemical components. *Chubu Forestry Res.* 67, 29–34. doi: 10.18999/chufr.67.29

Oka, A., Takahashi, J., Endoh, Y., and Seino, T. (2021). Bark effects on stemflow chemistry in a Japanese temperate forest I. The role of bark surface morphology. *Front. Forests Global Change* 4:654375. doi: 10.3389/ffgc.2021.654375

Pausas, J. G. (2015). Bark thickness and fire regime. *Funct. Ecol.* 29, 315–327. doi: 10.1111/1365-2435.12372

Rosell, J. A., Gleason, S., Méndez-Alonzo, R., Chang, Y., and Westoby, M. (2014). Bark functional ecology: Evidence for tradeoffs, functional coordination, and environment producing bark diversity. *New Phytol.* 201, 486–497. doi: 10.1111/nph.12541

Seino, T., and Endoh, Y. (2019). Ecological positions of conifers on the stand structure of the temperate forest in central Japan. *Chubu Forestry Res.* 67, 25–28. doi: 10.18999/chufr.67.25

Shibata, H., and Sakuma, T. (1996). Canopy modification of precipitation chemistry in deciduous and coniferous forests affected by acidic deposition. *Soil Sci. Plant Nutr.* 42, 1–10. doi: 10.1080/00380768.1996.10414683

Shibui, H., and Sano, Y. (2018). Structure and formation of phellem of Betula maximowicziana. *IAWA J.* 39, 18–36. doi: 10.1163/22941932-20170186

Shimaji, K., Sudo, S., and Harada, H. (1976). *Organization of Wood*. Tokyo: Morikita Publishing.

Simpson, M. G. (2019). *Evolution and Diversity of Vascular Plants. In Plant Systematics*, Third Edn. Cambridge, MA: Academic Press, 75–130.

Staelens, J., De Schrijver, A., and Verheyen, K. (2007). Seasonal variation in throughfall and stemflow chemistry beneath a European beech (Fagus sylvatica) tree in relation to canopy phenology. *Can. J. Forest Res.* 37, 1359–1372. doi: 10.1139/X07-003

Staelens, J., Houle, D., De Schrijver, A., Neirynck, J., and Verheyen, K. (2008). Calculating dry deposition and canopy exchange with the canopy budget model: review of assumptions and application to two deciduous forests. *Water Air Soil Pollut.* 191, 149–169. doi: 10.1007/s11270-008-9614-2

Trockenbrodt, M. (1990). Survey and discussion of the terminology used in bark anatomy. *IAWA Bull.* 11, 141–166. doi: 10.1163/22941932-90000511

Turpault, M. P., Kirchen, G., Calvaruso, C., Redon, P. O., and Dincher, M. (2021). Exchanges of major elements in a deciduous forest canopy. *Biogeochemistry* 152, 51–71. doi: 10.1007/s10533-020-00732-0

Van Stan, J. T., Dymond, S. F., and Klamerus-Iwan, A. (2021). Bark-water interactions across ecosystem states and fluxes. *Front. Forests Global Change* 4:660662. doi: 10.3389/ffgc.2021.660662

Van Stan, J. T., Lewis, E. S., Hildebrandt, A., Rebmann, C., and Friesen, J. (2016). Impact of interacting bark structure and rainfall conditions on stemflow variability in a temperate beech-oak forest, central Germany. *Hydrol. Sci. J.* 61, 2071–2083. doi: 10.1080/02626667.2015.1083104

Wetzel, S., Demmers, C., and Greenwood, J. S. (1989). Seasonally fluctuating bark proteins are a potential form of nitrogen storage in three temperate hardwoods. *Planta* 178, 275–281. doi: 10.1007/BF00391854

Wetzel, S., and Greenwood, J. S. (1989). Proteins as a potential nitrogen storage compound in bark and leaves of several softwoods. *Trees* 3, 149–153. doi: 10.1007/BF00226650

Wolterbeek, H. T., Verburg, P. K., Wamelink, G. W. W., and Van Dobben, H. (1996). Relations between sulphate, ammonia, nitrate, acidity and trace element

concentrations in tree bark in the Netherlands. *Environ. Monit. Assess.* 40, 185–201. doi: 10.1007/BF00414391

Xu, X., Yu, X., Mo, L., Xu, Y., Bao, L., and Lun, X. (2019). Atmospheric particulate matter accumulation on trees: A comparison of boles, branches and leaves. *J. Cleaner Produc.* 226, 349–356. doi: 10.1016/j.jclepro.2019.04.072

Zabel, R. A., and Morrell, J. J. (2020). "The decay setting: Some structural, chemical, and moisture features of wood features of wood in relation to decay development," in *Wood Microbiology*, Second Edn, eds R. A. Zabel and J. J. Morrell (Cambridge, MA: Academic Press), 149–183. doi: 10.1016/b978-0-12-819465-2.00006-1

Conflict of Interest: The authors declare that the research was conducted in the absence of any commercial or financial relationships that could be construed as a potential conflict of interest.